euspen's 25th International Conference & Exhibition, Zaragoza, ES, June 2025
www.euspen.eu

Novel in-situ measurement of microwave plasma temperature using laser absorption spectroscopy

Long Ye[1,#], Rui Zhang[2,#], Alasdair Mitchell[1], Adam Bennett[1], Chang Liu[2,*], Nan Yu[1,*]

[1]*Institute for Materials and Processes, The University of Edinburgh, Edinburgh, EH9 3FB, UK*
[2]*Institute for Imaging, Data and Communications, The University of Edinburgh, Edinburgh EH9 3JL, UK*

**Corresponding author: changliu@ed.ac.uk ; nan.yu@ed.ac.uk*
 # Joint first authors

Abstract
Microwave plasma figuring (MPF) has emerged as an advanced manufacturing technique for fabricating silica-based precision optics. This method employs a highly efficient and low-temperature plasma beam to selectively and locally remove materials with controlled precision, achieving surface form at the nanometer scale. Among the critical parameters influencing form accuracy, plasma jet temperature plays a pivotal role. This paper introduces a novel sensor-based in-situ method for measuring plasma jet temperature, leveraging laser absorption spectroscopy (LAS), which is a technique proven effective for capturing temperature distributions in combustion flames. A bespoke ring clamp, integrating light reflection mirrors and laser sensors, was developed to enable seamless integration with a machine tool. Preliminary experiments validate the feasibility of the developed LAS sensor system for accurately measuring absolute plasma temperatures, paving the way for enhanced control of material removal processes in MPF.

Plasma, in-situ measurement, laser absorption spectroscopy

1. Introduction

Microwave plasma figuring (MPF) is a key-enabling ultra-precision manufacturing technique for correcting form errors on optic surfaces [1, 2]. In this process, a high-density and low-temperature plasma beam, which consists of reactive species such as radicals, ions, and excited molecules, is generated at atmospheric pressure by microwave radiation (typically at 2.45 GHz). The confined plasma beam is then directed at the target surface, chemically etching the localized material by forming volatile byproducts. Thanks to these unique characteristics, the MPF becomes a promising alternative for fabricating large-scale and ultra-precision optical components.

In the MPF process, temperature plays a crucial role in determining the chemical reaction rates, plasma chemistry, and surface interactions, thereby ensuring efficient material removal and maintaining high surface quality. Traditional research often employed optical emission spectroscopy (OES) [3] to measure the plasma temperature. However, the OES measurement requires complex equipment setup and dedicated calibration, making it inappropriate for in-situ application. This paper proposes a novel integration of laser absorption spectroscopy (LAS) in a MPF machine tool for measuring the microwave plasma temperature distribution. The design of clamping the LAS sensor is articulated and demonstration of measurement results is presented.

2. LAS Measurement

2.1. Measurement principle

The LAS measurement principle [4] consists of a well-collimated laser at central frequency v [cm^{-1}] interacting with a target gas sample over a total path length of L [cm]. According to the Beer-Lambert law, a proportion of light is absorbed and the wavelength-dependent transmission coefficient τ_v is described as:

$$\tau_v = \left(\frac{I_t}{I_0}\right)_v = \exp\left(-P\int_0^L X_{abs}(x)S\big(T(x)\big)\Phi_v dl\right) \qquad (1)$$

where I_t and I_0 are the transmitted and incident laser intensities, respectively. P [atm] is the total pressure, T(x) [K] the local temperature, $X_{abs}(x)$ the local mole fraction of the absorbing species, Φ_v [cm] the line shape function and S(T) [$\mathrm{cm}^{-2}\mathrm{atm}^{-1}$] the temperature-dependent line strength of the transition. Given a uniform flow field over the laser path, the absorbance a_v can be defined as:

$$a_v = -\ln\tau_v = PX_{abs}\, S(T)\Phi_v L \qquad (2)$$

The scanned-wavelength method is implemented by acquiring the entire absorption feature through laser wavelength tuning over the target absorption transition. A polynomial baseline fit to the non-absorbing wings of transmitted laser intensity is first performed to extrapolate incident laser intensity in the absorbing frequency region. The absorbance is then acquired by taking the ratio between the incident and transmitted laser intensity.

As the line shape function Φ_v is normalized. i.e. $\int_{-\infty}^{+\infty}\Phi_v dv \equiv 1$, the integrated absorbance area A of the transition, which is defined as the area underneath the absorption lineshape function, is given by:

$$A = \int_{-\infty}^{\infty} a_v dv = PX_{abs}\, S(T)L \qquad (3)$$

According to the two-color strategy [5], the ratio of the integrated absorbance areas at two transitions, noted as A_1 and A_2, can be expressed as a function of the path-averaged temperature as below:

$$R = \frac{A_1}{A_2} = \frac{PX_{abs}\, S_1(T)L}{PX_{abs}\, S_2(T)L} = \frac{S_1(T)}{S_2(T)} \quad (4)$$

where the two lasers with different centre wavelengths are involved to measure the temperature of water vapour molecule.

2.2. Sensor system design

The LAS sensor system consists of a laser driver, an optical sensor, and a data acquisition (DAQ) unit, as depicted in Fig. 1.

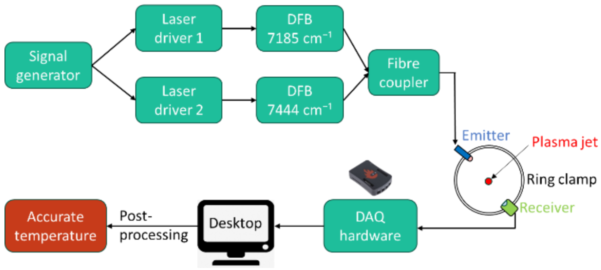

Figure 1. Design of LAS sensor system for measurement of plasma jet temperature.

The laser driving system is responsible for generating laser light of specific wavelength at the wavenumbers of 7185 cm^{-1} and 7444 cm^{-1} through the application of two distributed-feedback (DFB) laser diodes, NEL NLK1E5EAAA and NEL NLK1B5EAAA, respectively. The absorption features at these two wavelengths have been extensively applied in ratio thermometry, demonstrating proven sensitivity across the temperature range of 21°C to 1500°C. Each DFB laser diode is controlled in terms of temperature and current by a laser driver (Wavelength Electronics, LDTC 2-2E) to maintain the central wavenumber of each laser output. Low-frequency current modulation for both lasers is scanned using a 1 kHz sinusoidal wave. The two lasers are frequency division multiplexed to synchronize the optical signals. A dual-channel signal generator provides modulation frequencies at 100 kHz and 130 kHz to the two laser controllers. The optical sensors, consisting of an emitter and receiver, are both mounted at a ring clamp (as will be introduced in Section 2.3). Throughout the measurement process, the emitted light penetrates the plasma jet and the received signals will be captured by a Red Pitaya (RP)-based data acquisition (DAQ) system. The RP features analogue-to-digital converters (ADCs) operating at a sampling rate of 15.625 Mega Samples per second (MSps). The digitized signal is then demodulated using the integrated FPGA on the RP to obtain the $1f$ and $2f$ spectra, which are then transferred to a workstation via Ethernet.

2.3. Ring clamp

As illustrated in Fig. 2, a ring clamp which accommodates the optical sensors is developed, allowing for reliable measurement of microwave plasma temperature. In our MPF process, the plasma jet has a diameter of approximately 1 mm. To enhance the light interaction with the plasma and increase absorption, the optical ring is designed with multiple reflective mirrors to maximize the light path within the confined space and increase the amount of light passing through the plasma jet. As shown in Fig. 2(a), a C-lens collimator is used as the emitter to maintain the laser beam spot size within 1 mm after traveling 70 cm. A total of 26 right-angle reflective mirrors, each 3 mm in size, are arranged around a 41 mm diameter circle. The mirrors are coated with titanium and silicon dielectric layers to achieve 99.9% reflectivity at wavenumbers 7185 cm^{-1} and 7444 cm^{-1}. The mirrors are spaced 6° apart from each other. Once the light passes through the ring sensor, it creates a radial light distribution centered on the ring. The numbers on each mirror in Fig. 2(a) indicate the sequence in which the laser beam hits each mirror after being emitted by the collimator. The light is eventually detected by a small photodiode (Hamamatsu, G12182–010K), and a transimpedance amplifier is connected to the photodiode to convert the current signal into an amplified voltage signal. All components of the sensor are mounted on a 3D-printed prototype made from high-strength polycarbonate (PC) material to reduce distortion and deformation during testing, as shown in Fig. 2(b).

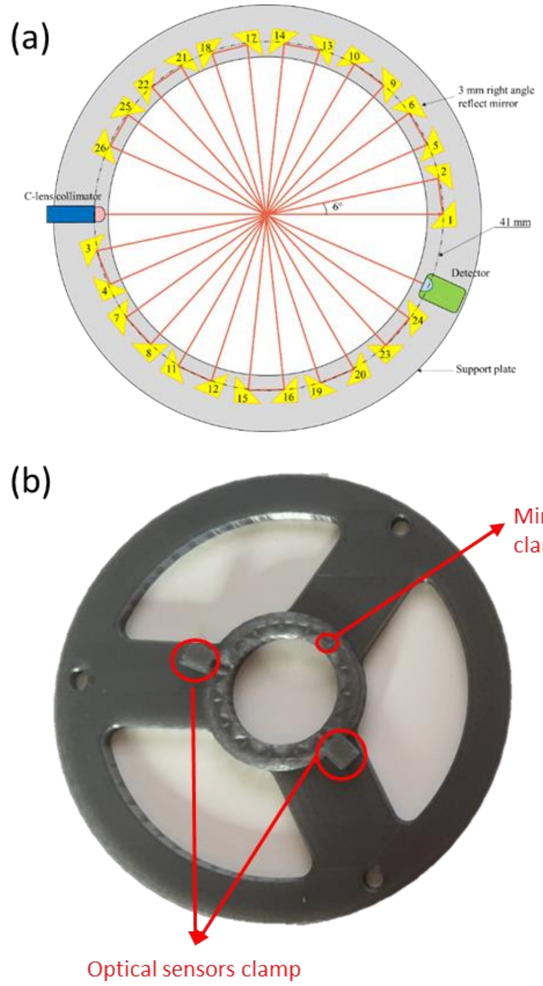

Figure 2. A ring clamp for alignment of mirrors for light reflection in respect to optical sensors: (a) design schematics and (b) 3D prototype.

3. Experimental setup

3.1. MPF machine tool

The plasma measurement experiment was conducted on the Satisloh® plasma polisher (SPP), as shown in Fig. 3(a).

Table 1 Parameter settings for plasma measurement experiments.

Plasma generator	Frequency/ MHz	2490
	Mean power/ W	15
	Pulse width/ µs	20
Gas supply	Iner gas (He)/ sccm	400
	Reactive gas (CF4)/ sccm	400
	Reactive gas (N2)/ sccm	400

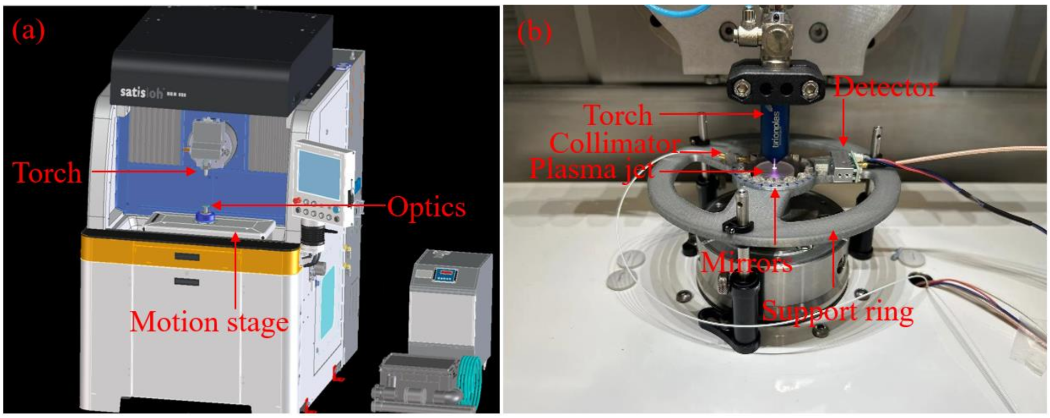

Figure 3. Experimental setup for plasma temperature measurement: (a) Satisloh® MPF machine tool and (b) the ring clamp integrated into the machine tool.

This machine utilizes a microwave plasma torch for precision optical polishing and figuring. A pulsed microwave plasma generator, whose tunable parameters are presented in Table 1, was used to create and sustain a plasma using high-frequency electromagnetic waves in the microwave range. The plasma torch is equipped with two-dimensional adjustment freedom and rotational capabilities, allowing for precise control during the polishing process. The nozzle of the torch, critical for plasma application, has a diameter of 1 mm. For the MPF process, helium was employed as inert gas to stabilize the plasma environment while nitrogen and carbon tetrafluoride were used as reactive gas to chemically etch silica-based materials.

3.2. Measurement setup

The support ring was securely mounted on the motion stage and aligned with the optics processing region of the SPP using three adjustable stand posts, as show in Fig. 3(b). The height of the sensing plane can be finely tuned using crimps on the posts, ensuring accurate positioning relative to the plasma region. Optical fibres and cables were neatly routed through a designated hole on the motion stage, extending to the bottom of the SPP and connected to laser driving and data acquisition devices positioned 1 meter away.

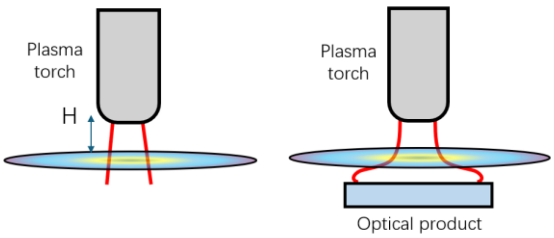

Figure 4. Comparative measurement without and with optical sample.

Two comparative experimental tests were conducted to assess the plasma torch performance. As demonstrated in Fig. 4, Test 1 varied the distance, denoted as H, between the nozzle plane and the laser plane. Temperature measurements were recorded at five distinct points when H was set to be 1 mm, 2 mm, 3 mm, 4 mm, and 5 mm, respectively, providing insight into the thermal gradient as a function of distance from the nozzle. Test 2 introduced a plano optical element beneath the plasma torch to simulate an optical figuring scenario. In this test, the optical element was positioned 3 mm below the torch nozzle, while the sensing plane was maintained 2 mm away from the nozzle, mimicking realistic operational conditions for plasma-assisted optical figuring. These tests are crucial for understanding how the plasma jet interacts with optical surfaces at varying distances, optimizing the process for precision applications. Note that the system was calibrated through estimating the ambient gas measurement, which was subsequently subtracted from the raw measurement results.

4. Results and discussion

Fig. 5 presents temperature measurements of a plasma jet over 30 seconds at different heights compared to the ambient temperature where no plasma is applied. The laser signal was originally captured in 1k Hz frame rate. However, to eliminate noise from unstable plasma species, measured signals were averaged 100 times before post-processing, resulting in an actual frequency of 10 Hz being displayed in Fig. 5. A detailed explanation of the signal post-processing can be found in [6].

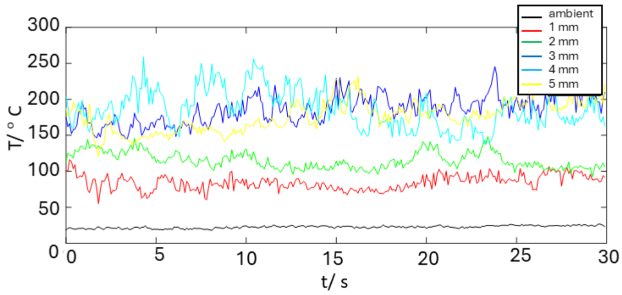

Figure 5. Temperature profiles of plasma jet within 30s at different H.

In general, the ambient temperature remains stable around 25°C, while the temperatures with plasma are significantly higher. At 1mm, temperatures fluctuate between 150°C and 190°C, gradually decreasing with height to around 100°C at 2 mm and 90°C to 120°C at 3 mm. At 4 mm and 5 mm, temperatures range between 90°C and 140°C, showing broader fluctuations than lower heights. The fluctuations in all datasets highlight the dynamic nature of plasma jets, though the noise has been effectively reduced by averaging. Overall, the data indicates a clear trend of decreasing temperature with height, which may require further investigation to understand fully.

Fig. 6 shows temperature measurements of a plasma jet over 30 seconds for two repetitive tests, denoted as "1" and "2", with ambient temperature as a reference. The aim of the tests was to assess the repeatability of temperature measurements using the sensor. The ambient temperature (black line) remains stable around 25°C, confirming a controlled environment. Both test "1" (red line) and test "2" (blue line) display similar temperature trends, fluctuating between 100°C and 140°C, though test "1" generally shows slightly higher readings, especially after the 10-second mark. Despite minor variations, both tests follow comparable patterns of peaks and valleys, suggesting consistent sensor performance. These fluctuations are typical of the dynamic behavior of plasma jets. The close alignment of the two tests indicates strong repeatability, with only small differences that fall within expected experimental variation. Overall, the sensor reliably captures the plasma jet's temperature across both trials, validating its use in future experiments requiring precise thermal monitoring.

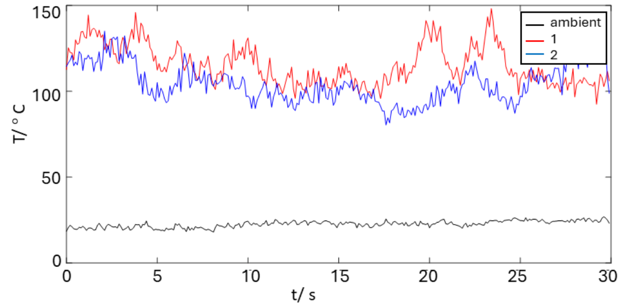

Figure 6. Repeatability test on the plasma temperature measurement.

Fig. 7 compares conditions with and without the presence of optics beneath the plasma. Two repetitive tests (labeled "With optics 1" in red and "With optics 2" in green) were conducted with optics present, while the "No optics 2 mm" test (blue line) represents the plasma jet without optics at 2 mm below the torch. The ambient temperature (black line) remains stable around 25°C. The presence of optics results in higher temperature fluctuations, with readings varying between 100°C and 200°C for both tests with optics. In contrast, the tests without optics show more stable temperatures, ranging between 75°C and 125°C, indicating a lower heat concentration when optics are absent. The consistent patterns between the two repetitive tests with optics suggest good repeatability, while the comparison between the "with optics" and "no optics" conditions highlights the significant thermal impact the optics have on the plasma jet environment. Overall, the data indicate that the introduction of optics beneath the plasma jet increases the measured temperature and induces more variability in the thermal profile.

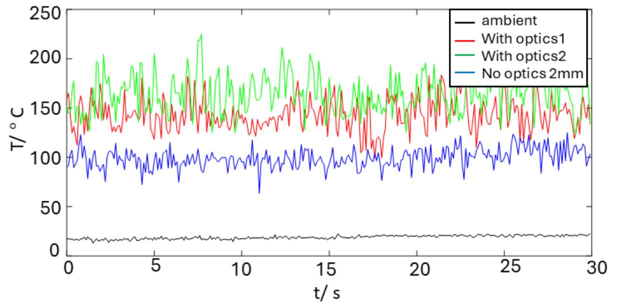

Figure 7. Comparison between temperature measurement with and without the presence of optics element.

5. Conclusion

This paper presents a novel portable sensor-based system based on laser absorption spectroscopy (LAS) for measuring the microwave plasma temperature distribution in situ. The design and prototype of the system, along with its integration into a functional microwave plasma figuring machine, were detailed. Initial experiments demonstrated that the LAS method effectively capture plasma temperature profiles with high repeatability. However, comparative tests revealed temperature fluctuations caused by exposure to the optical elements, which degraded measurement stability. These findings highlight the need for future work to optimize the design of the support ring structure, aiming to enhance measurement accuracy and overall system performance.

Acknowledgement

This work was supported by the EPSRC IAA (PV120 & PV203), the Royal Society (IEC\RC\213107) and the Royal Academy of Engineering (IF2223B-125). The authors would like to acknowledge the technical supports from Satisloh Group Gmbh.

References

[1] Nan YU, Jourdain R, et al. Investigation of a plasma delivery system for optical figuring process. Chinese Journal of Aeronautics. 2021 Apr 1;34(4):518-25.

[2] Mitchell A, Wei X, et al. A proposed methodology to develop digital twin framework for plasma processing. Results in Engineering. 2024 Dec 1;24:103462.

[3] Yuji T, Fujii S, et al. Optical emission characteristics of atmospheric-pressure nonequilibrium microwave discharge and high-frequency DC pulse discharge plasma jets. IEEE transactions on plasma science. 2009 May 5;37(6):839-45.

[4] Liu C, Xu L. Laser absorption spectroscopy for combustion diagnosis in reactive flows: A review. Applied Spectroscopy Reviews. 2019 Jan 2;54(1):1-44.

[5] Liu C, Cao Z, et al. Flame monitoring of a model swirl injector using 1D tunable diode laser absorption spectroscopy tomography. Measurement Science and Technology. 2017 Mar 3;28(5):054002.

[6] Xia J, Enemali G, et al. FPGA-accelerated distributed sensing system for real-time industrial laser absorption spectroscopy tomography at kilo-Hertz. IEEE Transactions on Industrial Informatics. 2023 Jul 24;20(2):2529-39.